Preclinical PET Study of Intravitreal Injections

Anxo Fernández-Ferreiro,[1–4] Andrea Luaces-Rodríguez,[1] Pablo Aguiar,[3,5] Juan Pardo-Montero,[3,6] Miguel González-Barcia,[2,4] Lara García-Varela,[3] Michel Herranz,[3,7] Jesús Silva-Rodríguez,[3] María Gil-Martínez,[8] María A. Bermúdez,[9] Alba Vieites-Prado,[10] José Blanco-Méndez,[1] María Jesús Lamas,[2,4] Francisco Gómez-Ulla,[8,11] Álvaro Ruibal,[3,5,12] Francisco Javier Otero-Espinar,[1] and Francisco González[8,11]

[1]Department of Pharmacology, Pharmacy and Pharmaceutical Technology and Industrial Pharmacy Institute, Faculty of Pharmacy, University of Santiago de Compostela, Santiago de Compostela, Spain
[2]Pharmacy Department, Complejo Hospitalario Universitario de Santiago (SERGAS), Santiago de Compostela, Spain
[3]Molecular Imaging Group, Complejo Hospitalario Universitario de Santiago (SERGAS), Health Research Institute of Santiago de Compostela (IDIS), Santiago de Compostela, Spain
[4]Clinical Pharmacology Group, Complejo Hospitalario Universitario de Santiago (SERGAS), Health Research Institute of Santiago de Compostela (IDIS), Santiago de Compostela, Spain
[5]Molecular Imaging Group, Department of Radiology, Faculty of Medicine, University of Santiago de Compostela, Spain
[6]Medical Physics Department, Complejo Hospitalario Universitario de Santiago (SERGAS), Santiago de Compostela, Spain
[7]Galician PET Radiopharmacy Unit, Galaria, Complejo Hospitalario Universitario de Santiago (SERGAS), Santiago de Compostela, Spain
[8]Service of Ophthalmology, Complejo Hospitalario Universitario de Santiago (SERGAS), Health Research Institute of Santiago de Compostela (IDIS), Santiago de Compostela, Spain
[9]Department of Animal Biology, Vegetal Biology and Ecology, Faculty of Biology, University of A Coruña, A Coruña, Spain
[10]Clinical Neurosciences Research Laboratory, Complejo Hospitalario Universitario de Santiago (SERGAS), Health Research Institute of Santiago de Compostela (IDIS), Santiago de Compostela, Spain
[11]Department of Surgery, University of Santiago de Compostela (CIMUS), Spain
[12]Nuclear Medicine Department, Complejo Hospitalario Universitario de Santiago (SERGAS), Santiago de Compostela, Spain

Correspondence: Francisco González, CIMUS, P0, D4, Universidad de Santiago de Compostela, Avd. Barcelona 22, E-15782 Santiago de Compostela, Spain; francisco.gonzalez@usc.es.
Francisco Javier Otero-Espinar, Faculty of Pharmacy, University of Santiago de Compostela, (USC) Pharmacy and Pharmaceutical Technology Department, Praza Seminario de Estudos Galegos s/n E-1570 Santiago de Compostela, Spain; francisco.otero@usc.es.

AF-F and AL-R contributed equally to the work presented here and should therefore be regarded as equivalent authors.

Submitted: March 6, 2017
Accepted: April 26, 2017

Citation: Fernández-Ferreiro A, Luaces-Rodríguez A, Aguiar P, et al. Preclinical PET study of intravitreal injections. *Invest Ophthalmol Vis Sci.* 2017;58:2843–2851. DOI:10.1167/iovs.17-21812

Purpose. This work aimed at describing the time course of vitreous clearance through the use of positron emission tomography (PET) as a noninvasive tool for pharmacokinetic studies of intravitreal injection.

Methods. The pharmacokinetic profile of intravitreal injections of molecules labeled with ^{18}Fluorine (^{18}F) was evaluated in adult Sprague Dawley rats by using a dedicated small-animal PET/computed tomography scanner. Different conditions were studied: three molecules radiolabeled with ^{18}F (^{18}F-FDG, ^{18}F-NaF, and ^{18}F-Choline), three volumes of intravitreal injections (7, 4, and 2 µL), and absence or presence of eye inflammation (uveitis).

Results. Our results showed that there are significant pharmacokinetic differences among the radiolabeled molecules studied but not among the injected volumes. The presence or absence of uveitis was an important factor in vitreous clearance, since the elimination of the drug was clearly increased when this condition is present.

Conclusions. Intravitreal pharmacokinetic studies based on the use of dedicated PET imaging can be of potential interest as noninvasive tools in ophthalmic drug development in small animals.

Keywords: intravitreal injection, radiolabeled molecules, vitreous clearance, intravitreal pharmacokinetics, PET

To date, most topical and systemic drugs have not achieved adequate therapeutic levels in the vitreous, mainly owing to the existence of different physiological barriers.[1] On one hand, topically instilled drugs are diluted by the tear film, thus causing significant drug loss in the lachrymal flow,[2] and furthermore their physicochemical characteristics must be adequate to cross the cornea.[3] On the other hand, the blood–retinal barrier (BRB), which comprises the retinal pigment epithelium and the tightly sealed walls of the retinal capillaries, complicates the arrival of systemic drugs to the vitreous.[4] For these reasons,

intravitreal administration has become an effective way to deliver drugs to the vitreous cavity, allowing high drug concentrations.[5]

To achieve a sustained therapeutic drug concentration in the vitreous, the frequency of administration should be based on the half-life of the drug ($t_{1/2}$). Regarding this question, several in vitro models have been proposed for the study of intravitreal pharmacokinetics, which take into account all aspects of the ocular anatomy and physiology.[6–9] However, one aspect that should be taken into consideration in the in vitro pharmacokinetic studies is the absence of convection,[10–13] even though the principal mechanism of transport through the vitreous is diffusion, and convection does not play a relevant role in the kinetics of small molecules. Other issues such as protein binding, melanin binding, drug metabolism, or active transport are usually not taken into account in the in vitro studies.[8,14] On the other hand, in vivo classical pharmacokinetic studies of intravitreal injections are limited because invasive techniques are involved.[15,16]

In recent years, molecular imaging techniques have become a turning point for the development and pharmacokinetic study of new drugs. These techniques involve noninvasive procedures in order to significantly decrease the number of animals used by increasing the number of measurements on each animal.[17,18] In particular for the field of intravitreal drugs, single photon emission computed tomography and magnetic resonance image (MRI) have been the most commonly used imaging techniques, mainly to study pharmacokinetics[14,19] and the release of drugs from implants and liposomes.[20–22]

However, in pharmacokinetic studies performed with MRI, the molecules used for the labeling of the drug usually have very high molecular weight, which can alter the properties of the original drug.[21]

The use of positron emission tomography (PET) has made it possible to label drugs with small β-emitting radioisotopes.[23] Current integrated PET/computed tomography (CT) scanners allow visualization of radiolabeled molecules by using a direct and noninvasive methodology, and the follow-up of the same subject over time to determine the pharmacokinetic properties of intravitreal injections.[24–26]

Different radionuclides can be used to elaborate radiotracers for PET scanning. The most commonly used radionuclides are typically isotopes with short half-lives such as ^{11}C, ^{13}N, ^{15}O, ^{18}F, ^{68}Ga, ^{82}Rb, or with longer half-lives such as ^{124}I or ^{89}Zr. ^{18}F is one of the most widely used because it is easily produced with a cyclotron, its positron energy of emission is 0.64 MeV, it is safe for patients, and it allows to obtain images with high resolution. Moreover, its half-life is long enough to be able to produce commercially manufactured fluorinated radiotracers at off-site locations and to be shipped to imaging services. In practice, ^{18}F radionuclide is linked to different molecules to achieve selective transport and distribution.[27]

Drug clearance in the vitreous can be influenced by various factors that include molecular weight, physicochemical properties of the drug, surgical procedure, injected volumes, and presence of ocular inflammation.[1] Also, the mechanisms of membrane transport and plasmatic clearance can highly influence the distribution and elimination of drugs after intravitreal administration. For this reason, fluorodeoxyglucose (^{18}F-FDG), ^{18}F-choline (^{18}F-Choline), and ^{18}F–sodium fluoride (^{18}F-NaF) were selected in our study because of their different molecular weight, polarity, and transport mechanism across biological membranes. The aim of the present work was to study the effect of some of these factors on the vitreous clearance by using dedicated PET/CT imaging techniques for in

Materials and Methods

Our work was designed as an experimental study in rats scanned in a dedicated PET/CT system after intravitreal injections of different radiolabeled molecules, different volumes, and absence/presence of inflammatory eye disease (uveitis).

Animals

This study was carried out on male adult Sprague Dawley rats with an average weight of 300 g, supplied by the animal facility of the University of Santiago de Compostela (Santiago de Compostela, Spain). During the experiments, the animals were kept in individual cages with free access to food and water in a room under controlled temperature (22°C ± 1°C) and humidity (60% ± 5%) and with day–night cycles regulated by artificial light (12/12 hours). The animals were treated as indicated in the ARVO Statement for the Use of Animals in Ophthalmic and Vision Research and according to the guidelines for laboratory animals.[28,29] Experiments were approved by the Galician Network Committee for Ethical Research and followed the Spanish and European Union (EU) rules (86/609/CEE, 2003/65/CE, 2010/63/EU, RD 1201/2005, and RD53/2013).

Intravitreal Injection Procedure

Intravitreal injection was performed according to the procedure described previously by Chiu et al.[30] Firstly, the animals were placed in a gas chamber containing 2% isoflurane in oxygen. When unconscious, the animals were removed from the chamber but kept under anesthesia with a mask (1.5% isoflurane in oxygen). The procedure was initiated by applying one drop of topical anesthesia (Colircusi Anestesico Doble: tetracaine 1 mg/mL and oxybuprocaine 4 mg/mL) on the eye followed by mydriatic eye drops (phenylephrine 100 mg/mL [Colircusi Fenilefrina] and tropicamide 10 mg/mL [Colircusi Tropicamide]) to visualize the eye fundus. Thereafter, radiolabeled molecules were injected into the vitreous through the pars plana by using a Hamilton syringe with a 34-G needle. The injection procedure was performed with a surgical microscope (Takagi OM-5 220-2; Takagi, Tokyo, Japan). Pictures of the procedure were taken by means of a digital camera (Nikon D-200; Nikon, Tokyo, Japan) attached to the microscope. Eyes with lens damage, or with significant bleeding when the intravitreal injection was made, were discarded from the study.

Experiments

The experiments were carried out by using intravitreal injections with three radiolabeled molecules and three different injection volumes, in healthy eyes and in eyes with lipopolysaccharide (LPS)–induced uveitis.

Effect of the Type of Injected Radiolabeled Molecules

Three different molecules were labeled with ^{18}F to evaluate the intravitreal pharmacokinetics. The radiolabeled molecules to be injected were ^{18}F-NaF, ^{18}F-FDG, and ^{18}F-Choline, with molecular weights of 41, 182, and 122 g/mol, respectively (Fig. 1).

The radioisotope $^{18}F^-$ was obtained from the nuclear reaction ^{18}O (proton, neutron) carried out in our PET Trace 800 cyclotron, according to the method described by Saha.[31] The radiosynthesis of ^{18}F-Na was made with a carbonate-type anion-exchange resin column, in such a way that the $^{18}F^-$ is

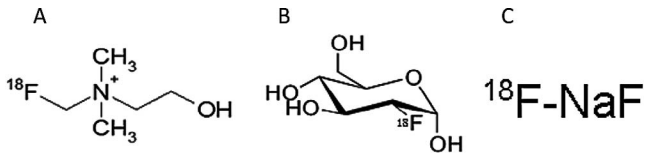

Figure 1. Chemical structure of (**A**) ^{18}F-Choline, (**B**) ^{18}F-FDG, and (**C**) ^{18}F-NaF.

fluoride by elution with potassium carbonate solution. ^{18}F-FDG and ^{18}F-Choline were produced on a TRACERlab MX synthesizer (GE Healthcare, Waukesah, WI, USA) by using cassettes and reagent kits from ABX (Advanced Biochemical Compounds, Radeberg, Germany). The nucleophilic substitution standard method was used in the case of ^{18}F-FDG and for the reaction of 18F-fluoromethyl triflate with dimethylethanolamine on a Sep-Pak column used in the case of ^{18}F-Choline.[32,33]

All procedures to obtain radiolabeled molecules were performed under good-manufacturing-practice conditions following the specific standards of European Pharmacopoeia.[34] The purity and stability quality control requirements were undertaken via high-pressure liquid chromatography/ion chromatography (930 Compact IC Flex con; Metrohm AG, Herisau, Switzerland) and thin layer chromatography. Osmolality (mOsm/kg) and pH were determined with a vapor pressure osmometer (VAPRO 5520; ELITECH Group, Paris, France) and a pH meter (WTW inoLab; WTW, Weilheim, Germany).

Effect of the Injected Volumes

The effect of the injected volume on the intravitreal pharmacokinetics of the abovementioned molecules was evaluated by using three different volumes: 2, 4, and 7 μL.

Effect of the Presence of Inflammation

Intravitreal pharmacokinetics was assessed in a uveitis animal model previously used by our group[33] and then compared to the intravitreal pharmacokinetics in healthy eyes. To induce uveitis, rats were inoculated into the right posterior paw with 1 mg/kg *Escherichia coli* LPS diluted in 0.1 mL phosphate-buffered saline by using a BD Micro-Fine syringe (BD, Oxford, UK) with 30-G needles. The presence of uveitis was assessed by direct inspection of the eye, using the surgical microscope. The animals were kept under such conditions for 24 hours. To reduce the number of animals, the influence of volume and presence or absence of uveitis were examined only for ^{18}F-NaF (monoexponential kinetics) and ^{18}F-FDG (biexponential kinetics). Four animals (eight eyes) were used in each condition studied.

Data Acquisition and Analysis

PET Data Acquisition. After the intravitreal injections of 1 MBq in each eye for all experimental conditions, dynamic PET acquisition was carried out to generate eight images of 15 minutes' duration for the first 1.5 hours. Afterwards, single PET images were obtained at 4 and 6 hours after drug administration. PET and CT images were acquired by using an Albira PET/CT Preclinical Imaging System (Bruker Biospin, Woodbridge, CT, USA). Animals were kept under anesthesia with a mask (1.5% isoflurane in oxygen). Respiration frequency and body temperature were monitored during the anesthesia period. The PET subsystem comprises three rings of eight compact modules based on monolithic crystals coupled to multianode photomultiplier tubes, forming an octagon with an axial field of view (FOV) of 40 mm per ring and a transaxial FOV of 80 mm in diameter. The CT system comprises a commercially available microfocus x-ray tube and a CsI scintillator 2D pixelated flat panel x-ray detector. Scatter and random coincidences were corrected by using the protocols implemented in the scanner. Attenuation correction was not performed. Images were reconstructed by using the maximum likelihood expectation maximization algorithm. Twelve iterations were performed with a reconstructed image pixel size of $0.4 \times 0.4 \times 0.4$ mm^3.

PET Data Analysis. After reconstruction, quantitative measurements were obtained by using the Amide's Medical Image Data Examiner.[35] Different regions of interest (ROIs) were manually drawn containing the signal on each eye. The ROIs were then replicated on the different temporal image frames to obtain the decrease curve of the radioisotope over time, conveniently corrected for radioactive decay.

Statistical Analysis. The curves of percentage of radiotracer in the eye versus time were fitted to the mono- and bicompartimental pharmacokinetic model by using nonlinear least squares regression analysis. The area under the percentage of radiotracer time curve AUC_0^{360} from zero to infinity was calculated by log-trapezoidal rule. The statistical analysis of experiments was performed by using a 1-way analysis of variance (ANOVA) and Tukey's multiple comparisons test. The nonlinear fitting and the statistical analysis were made by using the GraphPad Prism 6.0 software (2014; GraphPad Software, Inc., San Diego, CA, USA).

Results

All radiolabeled molecules were clearly detected in the vitreous cavity at the initial time of the study and it was possible to observe how the signal decreased over time. Figure 2 shows the coronal views of the fused PET/CT images from the initial frame (10 minutes after the injection) to the last frame (360 minutes after the injection).

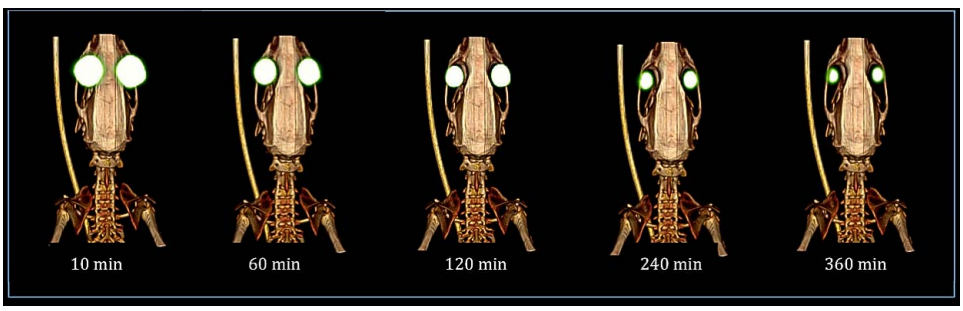

Investigative Ophthalmology & Visual Science

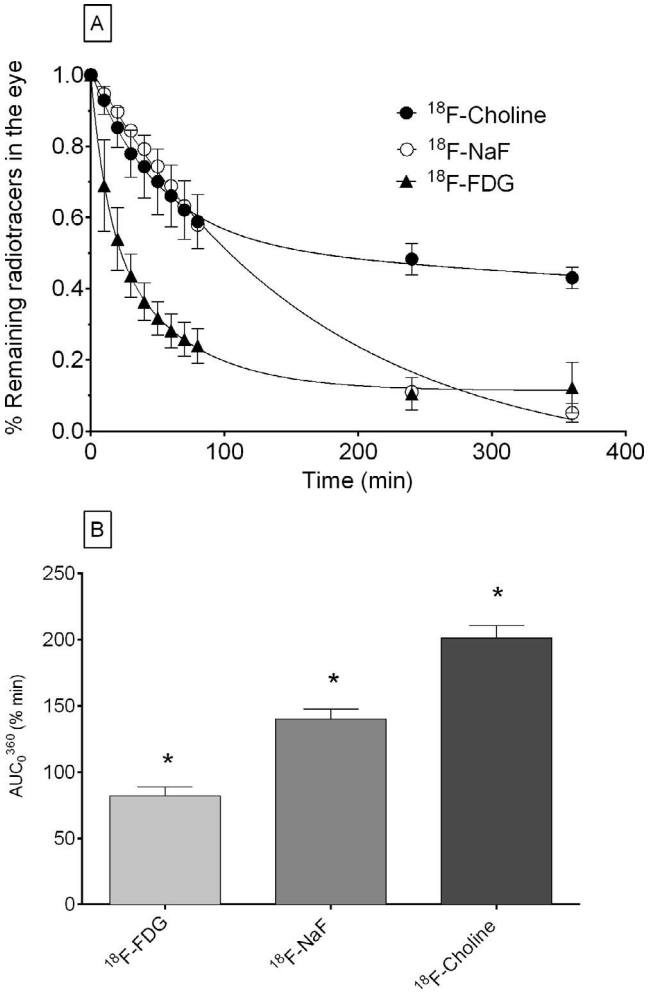

Figure 3. Influence of the drug type on its intravitreal release (mean ± SD, $n = 8$). (**A**) Intravitreal pharmacokinetic profile of ^{18}F-FDG, ^{18}F-NaF, and ^{18}F-Choline after intravitreal injection of 4 µL. (**B**) Representation of AUC_0^{360} (% min) for all radiotracers. *1-way ANOVA analysis and Tukey multiple comparison test show significant differences among the three different compounds ($\alpha < 0.01$).

Effect of the Type of Radiolabeled Molecules

The values measured from the ROI, containing each eye throughout time, were obtained for the three radiolabeled molecules, giving rise to significantly different kinetic curves (Fig. 3A). On the one hand, the clearance curves from ^{18}F-FDG and ^{18}F-Choline tracers appeared to fit a two-compartment model with a biphasic clearance from the vitreous. The obtained average intravitreal half-lives for these radiolabeled molecules were13.99 minutes for ^{18}F-FDG and 35.18 minutes for ^{18}F-Choline for the initial rapid elimination phase (α), and 214.2 minutes and 1351 minutes, respectively, for the slow elimination phase (β). Table 1 shows the pharmacokinetic parameters obtained by fitting the data to a bicompartmental model. On the other hand, the clearance curve from ^{18}F-Na showed a one-compartment pharmacokinetic model, and the average intravitreal half-life was 113.2 minutes. Table 2 shows the pharmacokinetic parameters obtained by fitting the data to a one-compartment pharmacokinetic model.

When comparing the area under the curve between 0 and 360 minutes (AUC_0^{360}) among three radiolabeled molecules, it was observed that ^{18}F-Choline remains significantly longer in the eye than ^{18}F-FDG and ^{18}F-NaF (Fig. 3B).

The radiolabeled molecules leave the eye and reach the systemic circulation, following different kinetic curves. Furthermore, the distribution at system level is also significantly different. Figure 4 shows that ^{18}F-NaF is captured by bone structures, while ^{18}F-FDG and ^{18}F-Choline are captured by internal organs.

The radiolabeled molecules used for the intravitreal injection had radiochemical purity for ^{18}F-FDG higher than 95% with a specific activity of approximately 1000 MBq/mL. The ^{18}F-Choline had radiochemical purity higher than 95% with a specific activity of approximately 500 MBq/mL. All radiotracers showed percentages of fluorine bound to the radiotracer that were higher than 95% at 8 hours post synthesis. The osmolality of all radiolabeled solutions was approximately 280 ± 10 mOsm/kg with a pH ≈7.4.

Effect of the Injected Volumes

Figure 5 shows no differences between the different volumes of intravitreal injections (2, 4, and 7 µL) for ^{18}F-Na and ^{18}F-FDG radioisotopes, which follow the same kinetics as previously described in Figure 3A. Tables 1 and 2 show that no statistically significant differences were found between pharmacokinetic parameters in relation to the injected volumes of both ^{18}F-FDG (Table 1) and ^{18}F-Na (Table 2). Finally, it should be noted that a transient vascular collapse in the retinal vessels was observed after administration of 7 µL, but not for 2 and 4 µL.

Effect of the Presence of Inflammation

Figure 6A shows that inflammation slightly, but with statistical significance, increased the vitreous clearance of ^{18}F-FDG. This effect was quantified by comparing the AUC_0^{360} of radiolabeled molecules in uveitis and under normal conditions. Figure 6B

Table 1. Pharmacokinetic Parameters Obtained by Fitting the Data to a Bicompartmental Model for ^{18}F-FDG and ^{18}F-Choline

	^{18}F-FDG				^{18}F-Choline
		4 µL*			
Pharmacokinetic Parameters	**2 µL***	**Normal†**	**Uveitis†**	**7 µL***	**7 µL**
α, min^{-1}	0.0336	0.03341	0.0416	0.0495	0.01970
$t_{1/2\alpha}$, min	20.65	20.75	16.66	13.99	35.18
B, min^{-1}	0.00285	0.002421	0.00218	0.00324	0.00051
$t_{1/2\beta}$, min	243.0	286.4	317.8	214.2	1351
AUC_0^{360}, % min	70.13 ± 5.31	88.15 ± 7.86	70.01 ± 5.70	82.05 ± 15.67	201.3 ± 18.83
R^2	0.9958	0.9958	0.9938	0.9963	0.9971

* No statistical differences for AUC_0^{360} (% min) were observed between different injection volumes (α not significant [n.s.]).

Table 2. Pharmacokinetic Parameters Obtained by Fitting the Data to Monocompartmental Model With ^{18}F-NaF

	^{18}F-NaF			
		4 µL*		
Pharmacokinetic Parameters	**2 µL***	**Normal†**	**Uveitis†**	**7 µL***
k, min^{-1}	0.00669	0.00656	0.00805	0.00612
$t_{1/2}$, min	103.6	105.7	86.11	113.2
AUC_0^{360}, % min	140.15 ± 14.93	135.23 ± 14.09	123.69 ± 21.09	137.03 ± 5.72
R^2	0.9982	0.9982	0.9952	0.9956

* No statistical differences were observed for AUC_0^{360} (% min) between different injection volumes (α n.s.).
† No statistical differences were observed for AUC_0^{360} (% min) between normal and uveitis eyes (α n.s.).

shows that eyes with uveitis had smaller AUC_0^{360} than normal eyes. In addition, statistically significant differences were found between the pharmacokinetic parameters in uveitis and normal conditions for the case of ^{18}F-FDG (Table 1). It must be mentioned that animals receiving an LPS injection developed a fibrinous reaction in the anterior chamber of the eye, which produced a pupillary membrane and an irregular pupil after drug-induced mydriasis, caused by the adhesion of the iris to the lens (Fig. 7). The uveitis model was successfully achieved in the same way as obtained in our previous studies.[36]

Discussion

Intravitreal injections are increasingly used in a multitude of retinal ophthalmic conditions such as age-related macular degeneration,[37] diabetic macular edema,[38] macular holes,[39] branch and central retinal vein occlusion,[40] and endophthalmitis.[41] The development of new intravitreal drugs or systems that modify their release involves wide preclinical development[42] in which pharmacokinetic studies play a key role.[43]

The use of small animals, such as Sprague Dawley rats, has many advantages because of their small size, the availability of research animal facilities, and multiple disease models suitable for them.[44,45] However, since they have a small vitreous volume, classic pharmacokinetic studies become difficult, with in vivo imaging being an ideal technique, as no invasive modalities are required to obtain experimental results.[46,47] To the best of our knowledge, our work is the first study of intravitreal pharmacokinetics with PET/CT in rats. Previous intravitreal pharmacokinetic studies have required larger

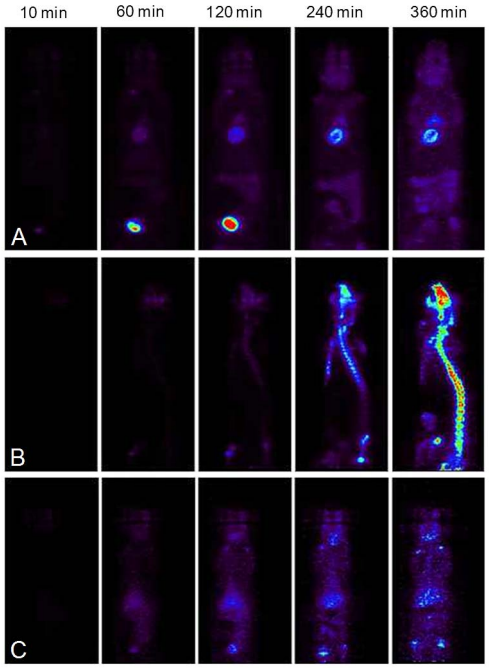

Figure 4. Representation of the systemic distribution of radiotracers at different times after intravitreal administration. (**A**) Coronal views after injection of ^{18}F-FDG. (**B**) Sagittal views after injection of ^{18}F-NaF.

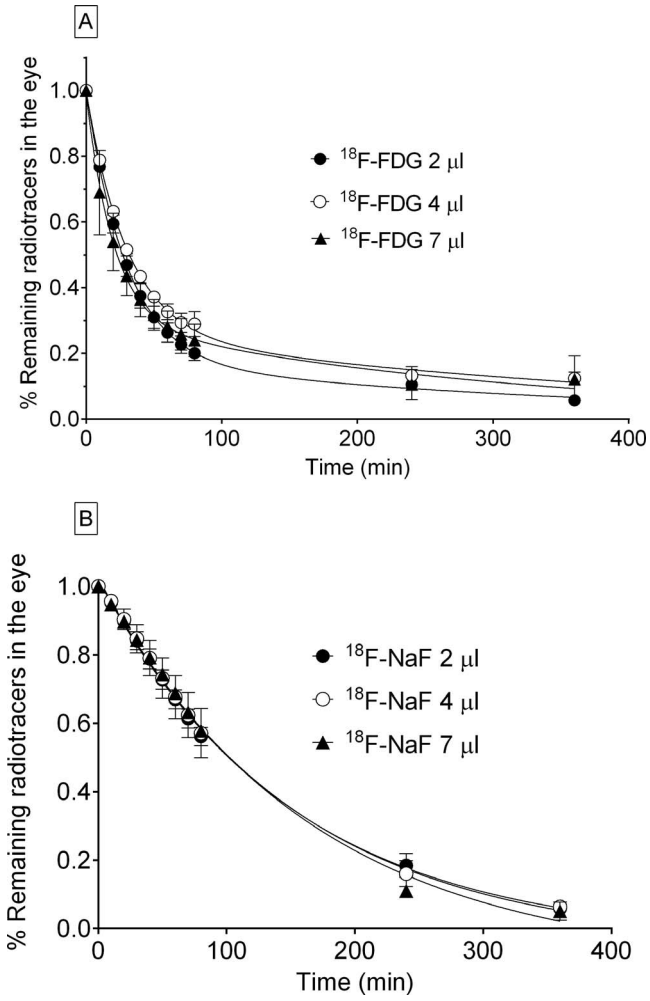

Figure 5. Influence of the injection volume on vitreal release (mean ± SD, $n = 8$). Intravitreal pharmacokinetic profile of ^{18}F-FDG (**A**) and

DOCKET ALARM

Explore Litigation Insights

Docket Alarm provides insights to develop a more informed litigation strategy and the peace of mind of knowing you're on top of things.

Real-Time Litigation Alerts

Keep your litigation team up-to-date with **real-time alerts** and advanced team management tools built for the enterprise, all while greatly reducing PACER spend.

Our comprehensive service means we can handle Federal, State, and Administrative courts across the country.

Advanced Docket Research

With over 230 million records, Docket Alarm's cloud-native docket research platform finds what other services can't. Coverage includes Federal, State, plus PTAB, TTAB, ITC and NLRB decisions, all in one place.

Identify arguments that have been successful in the past with full text, pinpoint searching. Link to case law cited within any court document via Fastcase.

Analytics At Your Fingertips

Learn what happened the last time a particular judge, opposing counsel or company faced cases similar to yours.

Advanced out-of-the-box PTAB and TTAB analytics are always at your fingertips.

API

Docket Alarm offers a powerful API (application programming interface) to developers that want to integrate case filings into their apps.

LAW FIRMS
Build custom dashboards for your attorneys and clients with live data direct from the court.

Automate many repetitive legal tasks like conflict checks, document management, and marketing.

FINANCIAL INSTITUTIONS
Litigation and bankruptcy checks for companies and debtors.

E-DISCOVERY AND LEGAL VENDORS
Sync your system to PACER to automate legal marketing.